

## Unexpected Four-Membered over Six-Membered Ring Formation during the Synthesis of Azaheterocyclic Phosphonates: Experimental and Theoretical Evaluation

Veronique Van Speybroeck,<sup>\*,†</sup> Kristof Moonen,<sup>‡</sup> Karen Hemelsoet,<sup>†</sup>  
Christian V. Stevens,<sup>\*,‡</sup> and Michel Waroquier<sup>†</sup>

Contribution from the Center for Molecular Modeling, Ghent University, Proeftuinstraat 86, B-9000 Ghent, Belgium, and Research Group SynBioC, Department of Organic Chemistry, Faculty of Bioscience Engineering, Ghent University, Coupure links 653, B-9000 Ghent, Belgium

Received December 12, 2005; Revised Manuscript Received April 26, 2006;

E-mail: veronique.vanspeybroeck@ugent.be; chris.stevens@ugent.be

**Abstract:** The cyclization of functionalized aminophosphonates is studied on both experimental and theoretical grounds. In a recently described route to phosphono- $\beta$ -lactams [Stevens C. V.; Vekemans, W.; Moonen, K.; Rammeloo, T. *Tetrahedron Lett.* **2003**, *44*, 1619], it was found that starting from an ambident allylic anion only four-membered rings were formed without any trace of six-membered lactams. New anion trapping experiments revealed that the  $\gamma$ -anion is highly reactive in intermolecular reactions. Ab initio calculations predict higher reaction barriers for the  $\gamma$ -anion due to restricted rotation about the C–N bond and due to highly strained transition states during ring closure. The sodium or lithium counterion, explicit dimethyl ether solvent molecules, and bulk solvent effects were properly taken into account at various levels of theory.

### 1. Introduction

Intramolecular ring-closure competition between a four-membered and a six-membered ring is generally accepted to lead to the six-membered ring.<sup>2</sup> Several ring-closure studies have been performed on the formation of lactones from  $\omega$ -bromoalkanoate ions to evaluate the influence of the ring size.<sup>3,4</sup> When the exo-tet situation is considered during ring closure,<sup>5</sup> the six-membered ring preference can be explained by a smaller Baeyer strain (angle strain) as well as a smaller Pitzer strain (due to eclipsed conformations of the hydrogens). The possibility to form a four- or a six-membered ring exists when an  $\alpha$ -alkenyl anion can ring close in an exo-tet mode either directly or through its mesomeric canonical form. However, a surprising preference for the formation of a four-membered ring was found during the synthesis of azaheterocyclic phosphonates.<sup>6–8</sup> When treated with a base, *N*-chloroacetyl-1-aminoalkenyl phosphonates derived from cinnamaldehyde exclusively lead to phosphono- $\beta$ -

lactams without any trace of the corresponding six-membered lactams. In a quite similar reaction where the anion was stabilized by a carbonyl group instead of a phosphonate group, the same experimental preference was observed toward the formation of the four-membered ring. However no explanation for this peculiar reactivity was given.<sup>9,10</sup> The higher reactivity of the  $\alpha$ -canonical anion compared to the  $\gamma$ -canonical anion could be believed to be important for the observed reactivity; however, steric factors may also play a role since exclusive  $\gamma$ -alkylation was observed using  $\beta,\gamma$ -unsaturated  $\alpha$ -silyloxyphosphonates.<sup>11</sup>

The main goal of the present paper is to unravel the origin of this remarkable selectivity toward four-membered ring formation. This is done both on experimental and theoretical grounds. In addition to the previously reported synthesis of 4-phosphono- $\beta$ -lactams new experiments were set up to trap the intermediate anions prior to cyclization to obtain information about the factors controlling the stability of the mesomeric resonance contributors. Further microscopic insight into stabilization and charge distribution is obtained by means of ab initio theoretical calculations.

The theoretical study of organometallic species as encountered here is challenging as the effects of the metallic counterion and solvent all contribute to the final reaction preference. To evaluate

<sup>†</sup> Center for Molecular Modeling.

<sup>‡</sup> Research Group SynBioC.

(1) Deleted in proof.

(2) Smith, M. B.; March, J. Kinetic Requirements for reactions. *Advanced Organic Chemistry*, 5th ed.; J. Wiley and Sons: New York, 2001; pp 278–282.

(3) Galli, C.; Illuminati, G.; Mandolini, L.; Tamborra, P. *J. Am. Chem. Soc.* **1977**, *99*, 2591–2597.

(4) Mandolini L. *J. Am. Chem. Soc.* **1978**, *100*, 550–554.

(5) Baldwin, J. E. *J. Chem. Soc., Chem. Commun.* **1976**, 734–736.

(6) Stevens, C. V.; Vekemans, W.; Moonen, K.; Rammeloo, T. *Tetrahedron Lett.* **2003**, *44*, 1619–1622.

(7) Moonen, K.; Laureyn, I.; Stevens, C. V. *Chem. Rev.* **2004**, *104*, 6177–6215.

(8) Moonen, K.; Stevens, C. V. *Synthesis* **2005**, 3603–3612.

(9) Bossio, R.; Marcos, C. F.; Marcaccini, S.; Pepino R. *Tetrahedron Lett.* **1997**, *38*, 2519–2520.

(10) Marcaccini, S.; Pepino, R.; Pozo M. C. *Tetrahedron Lett.* **2001**, *42*, 2727–2728.

(11) Hata, T.; Nakajima, M.; Sekine, M. *Tetrahedron Lett.* **1979**, 2047–2050.

the contribution of various parameters on the geometries, energies, and the reaction outcome, the reaction route was modeled in different environments: in the gas phase, with transmetalation with sodium or lithium as the counterion, and finally with inclusion of solvent interactions. The theoretical results are correlated with the experimental data.

From a theoretical point of view the stabilization of allylic anions by phosphorus substituents has attracted considerable interest.<sup>12–19</sup> The review of Katritzky<sup>20</sup> on the regioselectivity of reactions of heteroatom-stabilized allylic anions with electrophiles presents both experimental and theoretical considerations on this item. Unsymmetrically substituted allyl anions can react with electrophiles both intra- or intermolecularly at two sites, making these species of considerable importance. An early theoretical work on the stabilization of allylic anions by heteroatom-containing subgroups was presented by Denmark and Cramer where neutral, anionic, and lithiated P-allyl and P-methylphosphonic diamides were discussed.<sup>16</sup>

Recently, Pratt and co-workers performed several advanced calculations on the aggregation states of lithium carbenoids in the gas phase and in ethereal solvent.<sup>21</sup> From a methodological point of view, this work deserves attention as it incorporates the effects of the metallic cation which is further embedded in solution. It was explicitly shown that charge-separated species may be dramatically stabilized by solvent interactions. Pratt, Văn Nguyễn, and Ramachandran have additionally studied the performance of various electronic structure methods for the accurate reproduction of barrier heights for lithium enolates.<sup>22</sup> Recently, in a theoretical study performed by Ando, the origin of  $\pi$ -facial stereoselectivity in the alkylation of enolates was investigated.<sup>23</sup> In this study, the effects of the counterion, explicit coordination of solvent molecules with the lithium ion, and bulk solvent effects were found to be important for the reaction mechanism and energetics. Bearing this in mind, it is necessary to evaluate the influence of each of these effects on the reaction outcome for the present study.

The main motivation for studying the remarkable selectivity of the ring-closure reaction lies in the pharmaceutical importance of the  $\beta$ -lactam ring as part of several important antibiotics, including penicillin.<sup>24</sup> Also some electron-deficient monocyclic  $\beta$ -lactams appeared to be very active, including the commercially available azthreonam,<sup>25–28</sup> in which the  $\beta$ -lactam heterocycle

proved to be the key structural feature of this class of antibiotics. Furthermore, increasing resistance is a major threat in hospitals and in the community<sup>29</sup> and is mainly caused by the emergence and spread of  $\beta$ -lactamases, which are  $\beta$ -lactam-deactivating enzymes evolutionarily related to penicillin-binding proteins (PBPs).<sup>30–33</sup> Therefore, current research is focusing on new functionalized  $\beta$ -lactams having  $\beta$ -lactamase-inhibiting activity or combining antibacterial activity with enhanced stability toward  $\beta$ -lactamases.<sup>34,35</sup> In addition to these well-known antibacterial properties,  $\beta$ -lactams have also found application in inhibiting serine proteases. Members of this major class of enzymes are involved in numerous physiological processes including protein turnover, digestion, blood coagulation and wound healing, fertilization, cell differentiation and growth, cell signaling, the immune response, and apoptosis.<sup>36,37</sup>

## 2. Experimental and Calculation Methods

**General.** <sup>1</sup>H NMR spectra were recorded at 300 MHz with CDCl<sub>3</sub> as solvent and tetramethylsilane (TMS) as internal standard. <sup>13</sup>C NMR spectra were recorded at 75 MHz and <sup>31</sup>P NMR spectra at 121 MHz. MS spectra were measured using electron spray ionization (4000 V). THF was dried and distilled over sodium (benzophenone ketyl control). The absolute value of the coupling constants (*J*) in Hz and assignments of <sup>1</sup>H and <sup>13</sup>C peaks were determined using COSY, HSQC, HMBC, and DEPT experiments.

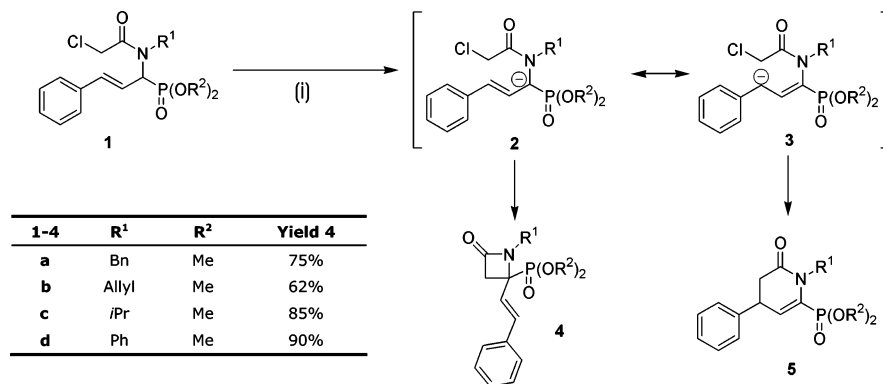
### Typical Procedure for the Synthesis of Phosphono- $\beta$ -lactams 4.

A NaH suspension [0.24 g (6 mmol, 1.2 equiv)] in mineral oil is washed three times with petroleum ether to remove the oil, and 15 mL of dry THF is added. Then, 5 mmol of the corresponding *N*-chloroacetyl amino alkenylphosphonate **1** in 5 mL of THF is added dropwise, and the reaction mixture is refluxed for 2 or 3 h protected from moisture with a CaCl<sub>2</sub> tube. After cooling, the mixture is poured into 25 mL of water and extracted with 20 mL of diethyl ether. The remaining water phase is then washed two times with 10 mL of diethyl ether. The combined organic phases are dried with MgSO<sub>4</sub>. The  $\beta$ -lactams are obtained in good purity after filtration and evaporation of the solvent. Further purification can be performed using column chromatography.

**Ab Initio Molecular Orbital Calculations.** All ab initio calculations were carried out with the GAUSSIAN 03 software package.<sup>38</sup> Density-functional theory (DFT) methods<sup>39</sup> have been shown to be more efficient than wave function based procedures such as highly correlated post-Hartree–Fock methods due to their excellent cost-to-performance ratio. Despite the importance of phosphorus compounds in chemistry, only limited levels of theory studies were conducted on such elements. The work of Leyssens and Peeters addresses the accuracy of various post-

- (12) Schleyer, P. V.; Clark, T.; Kos, A. J.; Spitznagel, G. W.; Rohde, C.; Arad, D.; Houk, K. N.; Rondan, N. G. *J. Am. Chem. Soc.* **1984**, *106*, 6468–6475.
- (13) Streitwieser, A., Jr.; Rajca, A.; McDowell, R. S.; Glaser, R. *J. Am. Chem. Soc.* **1987**, *109*, 4184–4188.
- (14) Denmark, S. E.; Dorow, R. L. *J. Am. Chem. Soc.* **1990**, *112*, 864–866.
- (15) Denmark, S. E.; Dorow, R. L. *J. Org. Chem.* **1990**, *55*, 5926–5928.
- (16) Denmark, S. E.; Cramer, C. J. *J. Org. Chem.* **1990**, *55*, 1806–1813.
- (17) Kranz, M.; Denmark, S. E. *J. Org. Chem.* **1995**, *60*, 5867–5877.
- (18) Koch, R.; Anders, E. *J. Org. Chem.* **1995**, *60*, 5861–5866.
- (19) (a) Leyssens, T.; Peeters, D. *J. Mol. Struct. (THEOCHEM)* **2004**, *673*, 79–86. (b) Leyssens, T.; Peeters, D. *J. Mol. Struct. (THEOCHEM)* **2004**, *686*, 71–82.
- (20) Katritzky, A. R.; Piffl, M.; Lang, H. Y.; Anders, E. *Chem. Rev.* **1999**, *99*, 665–722.
- (21) Pratt, L. M.; Streitwieser, A. *J. Org. Chem.* **2003**, *68*, 2830–2838.
- (22) Pratt, L. M.; Văn Nguyễn, N.; Ramachandran, B. *J. Org. Chem.* **2005**, *70*, 4279–4283.
- (23) Ando, K. *J. Am. Chem. Soc.* **2005**, *127*, 3964–3972.
- (24) Dürckheimer, W.; Blumbach, J.; Lattrell, R.; Scheunemann, K. H. *Angew. Chem.* **1985**, *24*, 180–202.
- (25) Imada, A.; Kitano, K.; Kintaka, K.; Muroi, M.; Asai, M. *Nature* **1981**, *289*, 590–591.
- (26) Sykes, R. B.; Cimarusti, C. M.; Bonner, D. P.; Bush, K.; Floyd, D. M.; Georgopadakou, N. H.; Koster, W. H.; Liu, W. C.; Parker, W. L.; Principe, P. A.; Rathnum, M. L.; Slusarchyk, W. A.; Trejo, W. H.; Wells, J. S. *Nature* **1981**, *291*, 489–491.

- (27) Gordon, E. M.; Ondetti, M. A.; Pluscec, J.; Cimarusti, C. M.; Bonner, D. P.; Sykes, R. B. *J. Am. Chem. Soc.* **1982**, *104*, 6053–6060.
- (28) Brogden, R. N.; Heel, R. C. *Drugs* **1986**, *31*, 96–130.
- (29) Neu, H. C. *Science* **1992**, *257*, 1064–1073.
- (30) Bulychev, A.; Massova, I.; Miyashita, K.; Mobashery, S. *J. Am. Chem. Soc.* **1997**, *119*, 7619–7625.
- (31) Golemi, D.; Maveyraud, L.; Vakulenko, S.; Tranier, S.; Ishiwata, A.; Kotra, L. P.; Samama, J.-P.; Mobashery, S. *J. Am. Chem. Soc.* **2000**, *122*, 6132–6133.
- (32) Meroueh, S. O.; Minasov, G.; Lee, W.; Shoichet, B. K.; Mobashery, S. *J. Am. Chem. Soc.* **2003**, *125*, 9612–9618.
- (33) Fisher, J. F.; Meroueh, S. O.; Mobashery, S. *Chem. Rev.* **2005**, *105*, 395–424.
- (34) Sandanayaka, V. P.; Prashad, A. S. *Curr. Med. Chem.* **2002**, *9*, 1145–1165.
- (35) Hammond, M. L. *J. Antimicrob. Chemother.* **2004**, *53*, Suppl. S2, ii7–ii9.
- (36) Bonneau, P. R.; Hasani, F.; Plouffe, C.; Malenfant, E.; LaPlante, S. R.; Guse, I.; Ogilvie, W. W.; Plante, R.; Davidson, W. C.; Hopkins, J. L.; Morelock, M. M.; Cordingley, M. G.; Deziel, R. *J. Am. Chem. Soc.* **1999**, *121*, 2965–2973.
- (37) Powers, J. C.; Asgian, J. L.; Ekici, O. D.; James, K. E. *Chem. Rev.* **2002**, *102*, 4639–4750.
- (38) Frisch, M. J.; et al. *Gaussian 03*; Gaussian, Inc.: Pittsburgh, PA, 2003.
- (39) Example of a reference work: Parr, R. G.; Yang, W. *Density-Functional Theory of Atoms and Molecules*; Oxford University Press: New York, 1989.

**Scheme 1.** Synthesis of 4-Phosphono- $\beta$ -lactams<sup>a</sup>

<sup>a</sup> Reagents and conditions: (i) 1.1 equiv NaH, THF,  $\Delta$ , 3 h.

Hartree–Fock and DFT methods on the geometries and energies of phosphorus-containing compounds.<sup>19</sup> The systems studied in that work are relatively small, and the use of highly correlated electronic structure methods such as MP2, MP4, QCISD, CCSD(T) was feasible. Their results show that the geometries resulting from DFT(B3LYP), MP2, and QCISD computations using the 6-31++g(d,p) are usually very close to each other. Another study by Pratt et al. revealed the structures of fluoromethylithium and chloromethylithium carbenoids in the gas phase and in ethereal solvent,<sup>40</sup> and it was found that the optimized geometries from the mPW1PW91/6-31+g(d) and QCISD/6-31+g(d) level agree to a large extent.

The systems of interest to the current work are too large to perform geometry optimizations at the post-Hartree–Fock level. DFT methods are therefore more suitable, and in the light of the previous discussion the B3LYP and mPW1PW91 exchange correlation functionals were selected to establish their influence on the geometry. The B3LYP functional is the most popular version of a hybrid DFT method combining the Becke exchange functional with the LYP correlation functional and which also contains 20% of exact Hartree–Fock exchange.<sup>41</sup> According to various references, the B3LYP methods provide excellent low-cost performance for geometry optimizations.<sup>42</sup> This is further confirmed by specific studies performed by Leyssens and Peeters on the properties of the phosphonate functional group.<sup>19</sup> The mPW1PW91 functional is also a hybrid functional containing 25% of exact exchange. The latter uses the modified Perdew–Wang exchange functional that has improved the long-range behavior as proposed by Adamo and Barone.<sup>43</sup> DFT models may substantially underestimate the activation energies for SN<sub>2</sub> substitution reactions. More information can be found in a study performed by Kormos and Cramer<sup>44</sup> where the relatively good performance of the mPW1PW91 functional is also shown. Another interesting paper within this respect is the study recently performed by Pratt and co-workers on the performance of various electronic structure methods for the evaluation of barrier heights for gas-phase reactions of lithium enolates.<sup>22</sup> They showed that when DFT methods succeeded in locating a transition-state structure, the geometries of the forming and breaking bond were in reasonable agreement with MP2 calculations. Also single-point MP2 energies at B3LYP geometries provide a reasonable estimate of the lithium enolate activation barriers in the gas phase. However, since the systems under consideration are quite large, such a strategy is computationally not feasible.

Another issue of importance is the basis set used for the calculations. As the present study involves anions, which have a more spread-out

electron density than neutral atoms, it is essential to add diffuse functions in the basis set.<sup>45</sup> The following basis sets were used: 6-31+g(d), 6-311 g(d,p), 6-311++g(d,p). The first one represents a double- $\zeta$  basis, whereas the others are triple- $\zeta$  basis sets. They further differ in the number of diffuse and/or polarization functions added.

The vibrational frequencies of the optimized structures were calculated at the same level of theory at which the geometries were optimized. The transition states were verified to have only one imaginary frequency and hence correspond to a first-order saddle point on the potential energy surface.

### 3. Experimental Results

The synthesis of the phosphono- $\beta$ -lactams under investigation was performed, starting from the appropriate *N*-chloroacetyl-1-amino alkenylphosphonates, **1**, which were obtained according to a literature procedure.<sup>6</sup> Upon treatment with a strong base, typically sodium hydride, a phosphorus-stabilized anion is formed, which can be represented by two canonical resonance contributors **2** and **3** (Scheme 1). The ring closure, performed in 3 h at 66 °C, showed that only one product was formed with a characteristic chemical shift between 24.01 and 24.75 ppm (<sup>31</sup>P NMR), while the chemical shift for a vinylic phosphonate is expected at significantly higher field (10–20 ppm). The same products were obtained at room temperature using LiHMDS as a base in diethyl ether as a solvent.

The proposed  $\beta$ -lactam structure was confirmed upon further spectroscopic investigation. The very high infrared absorption of the carbonyl ( $> 1750$  cm<sup>-1</sup>) is typical for highly strained rings. Furthermore, the ring CH<sub>2</sub>(3) appears as a second-order spin system in the <sup>1</sup>H NMR spectrum, involving a geminal coupling constant of 14.6–15.3 Hz and also quite large <sup>31</sup>P couplings (5.5–5.8 Hz), indicating the near presence of the phosphorus atom. According to the integral of the signals in the region of 6–7 ppm in the proton spectrum, two alkenyl protons are present in the molecule. A E-coupling of 16.2 Hz was found for all five products, next to smaller <sup>31</sup>P couplings. All aforementioned phosphorus couplings disappeared when the proton spectrum was run with selective <sup>31</sup>P decoupling. All <sup>13</sup>C peaks could be attributed to the appropriate carbon in the azetidines using 2D techniques (HSQC and HMBC) together with DEPT spectra. The quaternary carbon atom bearing the phosphonate group is expressed as a doublet ( $J = 166.7$ – $168.5$  Hz) in the <sup>13</sup>C spectrum, with a chemical shift clearly within the aliphatic

(40) Pratt, L. M.; Ramachandran, B.; Xidos, J.; Cramer, C. J.; Truhlar, D. G. *J. Org. Chem.* **2002**, *67*, 7607–7612.

(41) Becke, A. D. *J. Chem. Phys.* **1993**, *98*, 5648–5652.

(42) Coote, M. L. *J. Phys. Chem. A* **2004**, *108*, 3865–3872.

(43) Adamo, C.; Barone, V. *J. Chem. Phys.* **1998**, *108*, 664–675.

(44) Kormos, B. L.; Cramer, C. J. *J. Phys. Org. Chem.* **2002**, *15*, 712–720.

(45) Lynch, B. J.; Zhao, Y.; Truhlar, D. G. *J. Phys. Chem. A* **2003**, *107*, 1384–1388.

region (58.06–59.82 ppm). From this carbon, a clear HMBC coupling was observed with the  $CH_2(3)$  of the four-membered ring.

An overview of the regioselectivity of intermolecular reactions between heteroatom-stabilized allyl anions and electrophiles has been presented by Katritzky et al.<sup>20</sup> Even though an intramolecular reaction is considered in our system, some important directing factors could be identified such as nature of the counterion, reaction conditions, the nature of the electrophile, steric characteristics of the anion and the electrophile, coordination between the electrophile and the substrate prior to bond formation, etc. Lithium and sodium have been evaluated as counterions giving the same selectivity. The reaction conditions, on the other hand, have an influence on the reaction rate but not on the selectivity. Formation of the anion occurs fast and can be followed visually by the evolution of hydrogen gas from the reaction mixture upon addition of sodium hydride at room temperature. After the  $H_2$ -gas evolution ceases, the reaction needs a further 3 h of reflux in THF (bp 66 °C), while the reaction did not complete during an overnight reflux period in diethyl ether (bp 35 °C). The high number of functionalities in the substrate calls for a more profound investigation of other determining factors. Furthermore, the intramolecular reaction under investigation involves additional complications compared to the intermolecular reactions, such as anion geometry and substrate conformation.

A phosphonate group is known to greatly stabilize carbanions in the  $\alpha$ -position through electrostatic interactions.<sup>15,20</sup> This might explain the lack of reactivity in the  $\gamma$ -position. To study the selectivity of the reaction, an experiment was set up to trap the allyl anion with common electrophiles, such as a proton (or a deuteron) or methyl iodide. For this purpose, *N*-acetyl-1-amino alkenylphosphonate, **8**, was synthesized using a modified procedure. Imine **6** was phosphorylated regioselectively using dimethyl phosphite in methanol (97% yield),<sup>46</sup> and the resulting aminophosphonate **7** was then acetylated using acetyl chloride and DMAP/pyridine (63% overall yield). The resulting *N*-acetyl-1-amino alkenylphosphonate, **8**, is sterically and electronically very similar to the *N*-chloroacetyl substrates but is not prone to intramolecular reactions because of the lack of a leaving group. Initial attempts to prepare the anion with LiHMDS and to trap it with methyl iodide resulted in complex mixtures. When the anion was quenched with water, an unseparable mixture of starting material and two new products was found in low yield after extraction. The generation of several side products was probably induced by the acidic acetyl protons leading to unselective deprotonation by LiHMDS. However, when sodium hydride was used instead, deprotonation proceeded selectively, and a clean mixture of starting material **8** and its isomer **10** was found after quenching with water. Furthermore, both isomers could be separated using column chromatography, which allowed the unambiguous determination of the structure of the resulting isomer with the use of selected NMR techniques.

The ratio of both isomers was rather surprisingly in favor of the  $\gamma$ -protonated isomer **10**, suggesting it as an important contributor to the canonical resonance system of the allyl anion. When deuterium oxide was used to quench the allyl anion, the corresponding monodeuterated products were obtained in the

same ratio. The reaction was then repeated under the same conditions, however, using methyl iodide as an intermediate soft electrophile. This might provide a better model for the intramolecular alkylation. In this case, the  $\gamma$ -methylated product **11** was formed as a mixture of (*E,Z*)-isomers ( $\delta^{31P} = 16.3$  and 16.2). Purification using column chromatography or crystallization failed. The structure was confirmed, however, by comparing the  $^{13}C$ ,  $^{31}P$ , and DEPT spectra from the crude reaction mixture with vinyl phosphonate **10** and by determining its mass spectrum using LC-MS. No other phosphorus-containing compounds were detected using  $^{31}P$  NMR.

The results obtained from the intermolecular reactions with allylic anion **9** are in contradiction with the exclusive  $\beta$ -lactam formation in the intramolecular reaction. To elucidate these peculiarities, ab initio molecular orbital calculations were performed as presented in the following section, giving microscopic insight into the reaction preference.

#### 4. Ab Initio Results

**Free Anions.** The energetically most favored structure of the free carbanion is visualized in Figure 1 (labeled as **2a** in Scheme 1). This structure was found by applying various internal rotations about single bonds and selecting stepwise the most stable conformation along the rotational potential. For the discussion of the geometry some of the carbon atoms are labeled as shown in Figure 2 (Anion I). The most important geometrical parameters are listed in Table 1.

One particular internal rotation deserves special attention, i.e., about the  $C_1-C_2$  bond, as it gives rise to either the *E* or *Z* geometry of the  $\gamma$ -anionic form ( $\alpha$  and  $\gamma$  refer to the phosphorus atom). The *E* geometry cannot lead to six-membered rings. The latter conformer was found to be highly unstable (14.8 kJ/mol), indicating that the *Z* geometry is preferred which can either close at the  $\gamma$ - or  $\alpha$ -position.

Within the context of a further cyclization toward four- or six-membered ring formation, the  $C_5-C_1$  and  $C_5-C_3$  distances are relevant, as they represent the distances from the  $\alpha$ - and  $\gamma$ -carbon centers of the allylic unit to the chlorinated carbon atoms. They amount to 2.78 and 3.65 Å, respectively, and indicate that the most stable conformer of the anion has a characteristic geometry that is suitable for four-membered ring formation. Also, the internal rotation about the  $C_1-N$  bond, will play a crucial role in the reaction mechanism, as it determines the relative position of the chlorinated carbon atom ( $C_5$ ) toward the  $\alpha$ - or  $\gamma$ -carbon center (respectively,  $C_1$  or  $C_3$ ). In the energetically most favored conformation the dihedral angle  $C_2C_1NC_4$  amounts to  $-82.19^\circ$ , and  $C_5$  points away from the carbon atom at the  $\gamma$ -position of the phosphorus (cf. Figure 1).

To unravel the mechanism of the further ring closure, it is instructive to study the polarization of charge of the carbanion. Therefore, we calculated partial atomic charges according to the ChelpG scheme<sup>47</sup> on the optimized geometries. The latter method uses electrostatic derived charges and has proven its accuracy for calculating atomic populations.<sup>48,49</sup> The results are given in Table 2. The phosphorus atom has a highly positive charge (0.88), whereas the negative charge is delocalized over the allyl unit with a slight polarization toward the  $\gamma$ -carbon atom

(46) Van Meenen, E.; Moonen, K.; Acke, D.; Stevens, C. V. *Arkivoc* **2006**, 31–35.

(47) Breneman, C. M.; Wiberg, K. B. *J. Comput. Chem.* **1990**, *11*, 361–373.

(48) Sigfridsson, E.; Ryde, U. *J. Comput. Chem.* **1998**, *19*, 377–395.

(49) Martin F.; Zipse, H. *J. Comput. Chem.* **2005**, *26*, 97–105.

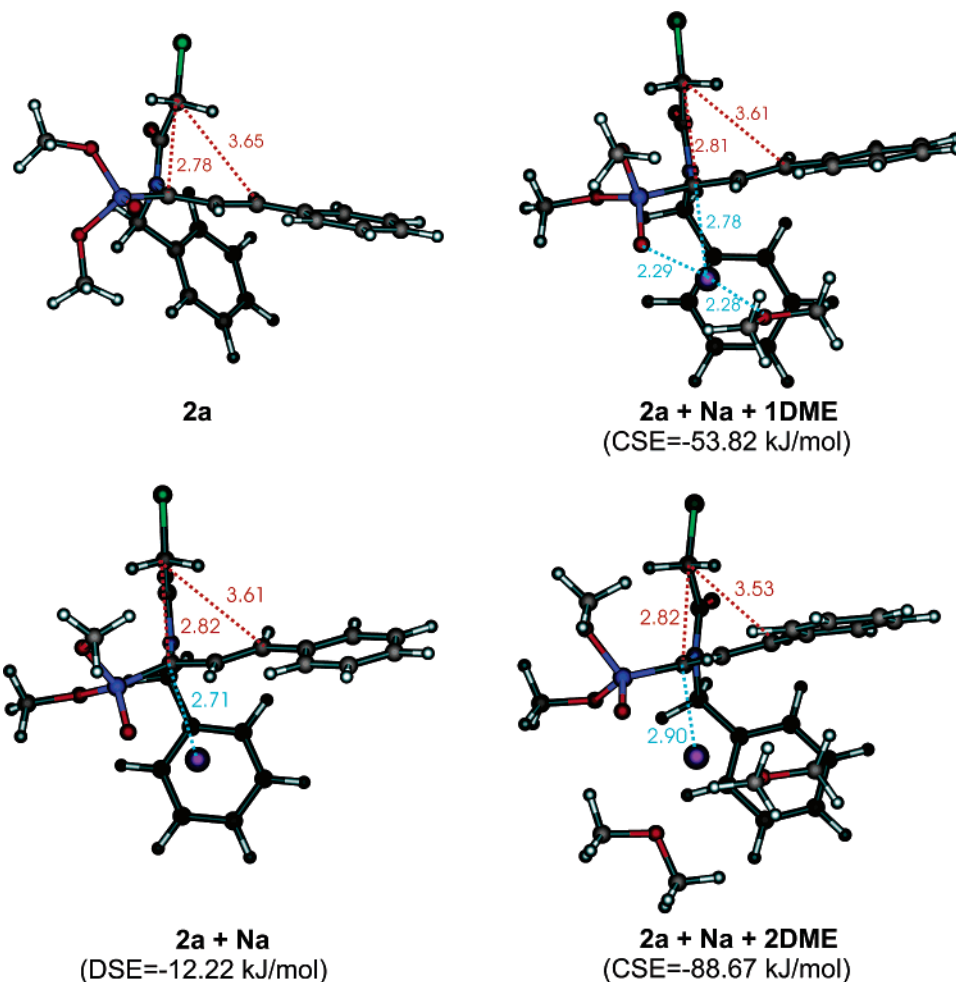


**Figure 1.** Optimized conformers of the anions in different molecular environments: **2a** in the gas phase, **2a** + Na including one sodium ion, **2a** + Na + 1DME and **2a** + Na + 2DME including one sodium ion and one or two DME molecules. All optimizations are performed at the B3LYP/6-31+g(d) level.

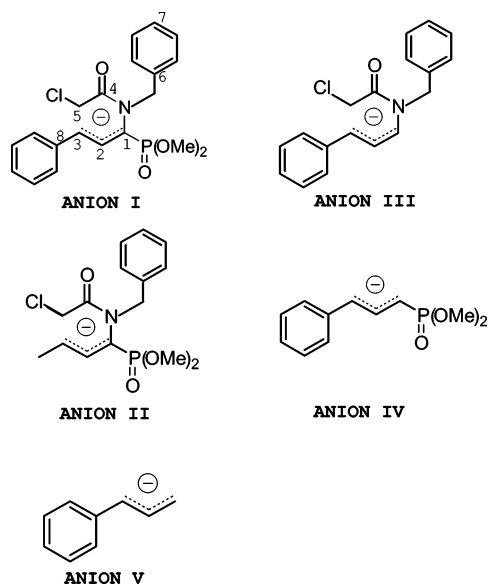


**Figure 2.** Allyl stabilized carbanions.

(C<sub>3</sub>). Also, the oxygen of the P=O bond carries a large negative charge and is the basic reason for the positively charged phosphorus atom. The origin of this charge distribution is studied more in detail by calculating the energetically most favored structure of some other free anions with different substitution

patterns (cf. Figure 2). It turns out that the net amount of negative charge on the allyl unit systematically increases by removing the phosphonate group and/or the nitrogen centered group (Anion III, Anion IV, Anion V). In the presence of the phosphonate group (Anion IV) a highly polarized carbon–phosphorus bond is obtained with a large positive charge (1.12) on the P atom. Previous results are in accordance with the findings of Cramer and Denmark.<sup>16</sup>

**Protonation Energies.** The reactivity of the  $\alpha$ - and  $\gamma$ -carbon atoms ( $\alpha$  and  $\gamma$  are referred with respect to the phosphonate group) toward electrophilic attack can be estimated by calculating the protonation energies at both carbon positions (see Scheme 2):

$$\Delta E_x = E(\text{Anion} + H_x) - E(\text{Anion}) - E(H^+) \quad (1)$$

with  $x = \alpha$  or  $\gamma$ . In Scheme 2, the  $\alpha$ - and  $\gamma$ -protonated forms are related to **8** and **10**, respectively. The results are shown schematically in Figure 3. For the Anions I and II having both the phosphonate group and the nitrogen-containing subgroup, the protonated molecule at the  $\gamma$ -position is more stable by 23 and 37 kJ/mol, respectively. When removing either the phosphonate or nitrogen centered subgroup, the stability sequence inverts. These findings are in accordance with the experiments described in the previous section: the  $\gamma$ -carbon has a larger proton affinity than the  $\alpha$ -carbon. However, these thermody-

**Table 1.** Most Important Geometrical Characteristics of Reactants and Transition States at the B3LYP/6-31+g(d) level<sup>a</sup>

Gas Phase Structures			
	Anion I (2a)	TS4	TS6
C <sub>5</sub> –C <sub>1</sub>	2.7762	2.1233	2.8210
C <sub>5</sub> –C <sub>3</sub>	3.6454	3.7046	2.5544
C <sub>1</sub> –C <sub>5</sub>	1.8131	2.4117	2.3520
C <sub>3</sub> C <sub>2</sub> C <sub>1</sub> N	0.34	9.27	–1.32
C <sub>2</sub> C <sub>1</sub> NC <sub>4</sub>	–82.19	–116.51	–36.02
C <sub>1</sub> NC <sub>4</sub> C <sub>5</sub>	–1.11	10.28	–15.24
Transmetalated Structures			
	Anion I +Na	TS4 + Na	TS6 + Na
C <sub>5</sub> –C <sub>1</sub>	2.8176	1.9825	2.7987
C <sub>5</sub> –C <sub>3</sub>	3.6139	3.6417	2.1833
C <sub>1</sub> –C <sub>5</sub>	1.7986	2.4820	2.4213
C <sub>3</sub> C <sub>2</sub> C <sub>1</sub> N	–4.41	6.59	–2.25
C <sub>2</sub> C <sub>1</sub> NC <sub>4</sub>	–80.36	–117.36	–31.36
C <sub>1</sub> NC <sub>4</sub> C <sub>5</sub>	2.86	11.28	–16.72
Na–C <sub>1</sub>	2.7097	2.9223	2.8038
Na–C <sub>3</sub>	3.5203	2.7938	2.7610
Na–C <sub>6</sub>	2.8747	2.7873	2.7168
Na–C <sub>7</sub>	2.9833	3.6904	3.0384
	Anion I +Li	TS4 + Li	TS6 + Li
C <sub>5</sub> –C <sub>1</sub>	2.8327	1.9674	2.7920
C <sub>5</sub> –C <sub>3</sub>	3.6866	2.8895	2.4085
C <sub>1</sub> –C <sub>5</sub>	1.7986	2.4902	2.4432
C <sub>3</sub> C <sub>2</sub> C <sub>1</sub> N	–2.08	5.93	–1.64
C <sub>2</sub> C <sub>1</sub> NC <sub>4</sub>	–83.80	–120.25	–31.42
C <sub>1</sub> NC <sub>4</sub> C <sub>5</sub>	2.53	11.08	–16.28
Li–C <sub>1</sub>	2.3744	2.5211	2.4360
Li–C <sub>3</sub>	3.6033	2.5803	2.4183
Li–C <sub>6</sub>	2.4987	2.5595	2.3279
Li–C <sub>7</sub>	2.7311	3.7625	2.7642
Transmetalated Structures Coordinated with Dimethylether Molecules			
	Anion I + Na+1DME	TS4 + Na + 1DME	TS6 + Na + 1DME
C <sub>5</sub> –C <sub>1</sub>	2.8142	1.9995	2.7905
C <sub>5</sub> –C <sub>3</sub>	3.6081	3.6616	2.2261
Cl–C <sub>5</sub>	1.7994	2.4685	2.4100
C <sub>3</sub> C <sub>2</sub> C <sub>1</sub> N	–5.12	5.23	–2.68
C <sub>2</sub> C <sub>1</sub> NC <sub>4</sub>	79.53	–116.69	–31.66
C <sub>1</sub> NC <sub>4</sub> C <sub>5</sub>	2.47	10.87	–17.73
Na–C <sub>1</sub>	2.7773	3.0057	2.6789
Na–C <sub>3</sub>	3.5396	2.8753	3.8638
Na–C <sub>6</sub>	3.0571	2.9603	2.7726
Na–C <sub>7</sub>	3.2443	3.8839	3.5234
Na–O <sub>1</sub>	2.2795	2.2779	2.2758
O <sub>1</sub> –C <sub>6</sub>	5.0397	5.1811	4.7951
O <sub>1</sub> –C <sub>8</sub>	4.4539	4.3069	5.0642

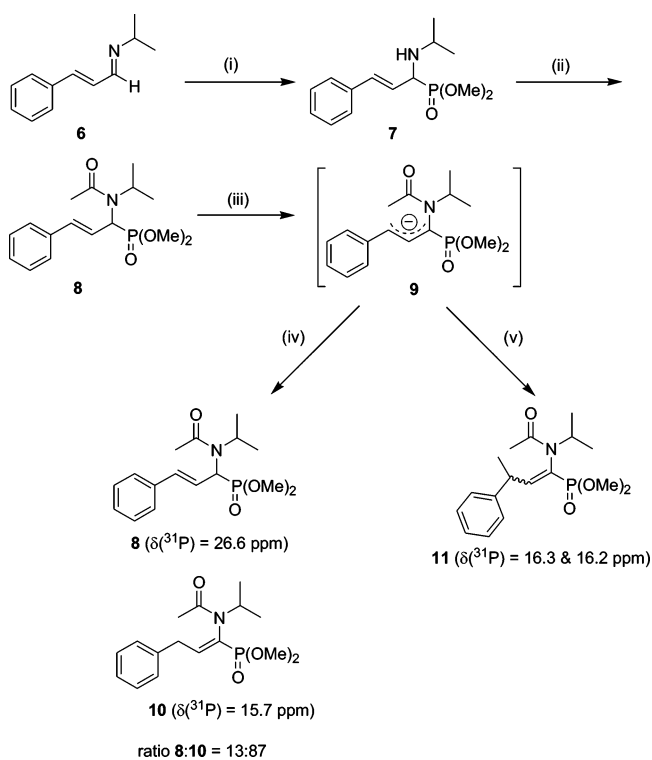
<sup>a</sup> All distances are reported in Å, angles and dihedrals in degrees. O<sub>1</sub> is the oxygen of the DME molecule.

namic findings cannot explain the exclusive reaction toward four-membered rings. Most probably the transition state toward six-membered ring formation is characterized by energetically unfavorable effects, which inhibit the ring closure at the  $\gamma$ -site.

**Transmetalation.** Although the free gas-phase anions provide useful information, the counterion may contribute to the factors that affect the regioselectivity of heteroatom-stabilized allylic anions. Therefore, the free anion with the presence of a sodium counterion was optimized. Various stable structures were obtained when starting from different initial positions of the sodium cation. The most stable configuration is visualized in Figure 1 (labeled as **2a**+Na). The sodium counterion prefers a position between the allylic subsystem and the benzyl group

**Table 2.** Atomic Charges Calculated According to the ChelpG Scheme at the B3LYP/6-31+g(d) Level of Theory for Various Anions

	anion I (2a)	anion II	anion III	anion IV	anion V
C <sub>5</sub>	0.21	0.13	0.30		
Cl	–0.29	–0.29	–0.31		
C <sub>1</sub>	–0.39	–0.32	–0.43	–0.63	–0.75
C <sub>2</sub>	0.10	–0.15	0.11	0.24	0.28
C <sub>3</sub>	–0.47	–0.20	–0.55	–0.59	–0.66
N	0.20	0.15	0.23		
P	0.88	0.89		1.12	
O	–0.65	–0.67		–0.70	
	anion I + Na	anion I + Li	anion I + Na+1DME	anion I + Na+2DME	
C <sub>5</sub>	–0.05	0.03	0.03	0.06	
Cl	–0.20	–0.21	–0.22	–0.22	
C <sub>1</sub>	–0.34	–0.42	–0.34	–0.30	
C <sub>2</sub>	0.04	0.01	0.09	0.10	
C <sub>3</sub>	–0.51	–0.40	–0.47	–0.49	
N	–0.04	0.02	–0.01	–0.02	
P	0.81	0.96	0.80	0.83	
O	–0.64	–0.69	–0.70	–0.61	
Na/Li	0.59	0.54	0.55	0.49	
O <sub>1</sub>			–0.36	–0.20	
O <sub>2</sub>			–	–0.19	

**Scheme 2<sup>a</sup>**

<sup>a</sup> Reagents and conditions: (i) 2 equiv HPO(OMe)<sub>2</sub>, MeOH,  $\Delta$ , 3 h; (ii) 1.5 equiv AcCl, 0.2 equiv DMAP, 2 equiv pyridine, THF, rt (1 h),  $\Delta$  (1 h); (iii) 1) 1.1 equiv NaH, –78 °C, THF; 2) –78 °C  $\rightarrow$  rt (2h); (iv) H<sub>2</sub>O, 2 h, rt; (v) 3 equiv MeI, 2 h, rt.

(cf. Table 1: Na–C<sub>1</sub> = 2.71 Å, Na–C<sub>6</sub> = 2.87 Å, Na–C<sub>7</sub> = 2.98 Å). The sodium atom makes an additional contact with the oxygen of the P=O bond (Na–O = 2.27 Å). The lithiated anions have similar geometrical characteristics (cf. Table 1: Li–C<sub>1</sub> = 2.37 Å, Li–C<sub>6</sub> = 2.50 Å, Li–C<sub>7</sub> = 2.73 Å). The atomic charges are not drastically altered by incorporating the counterion (cf. Table 3). For further cyclization, it is also important to analyze the effect of the counterion with respect to the

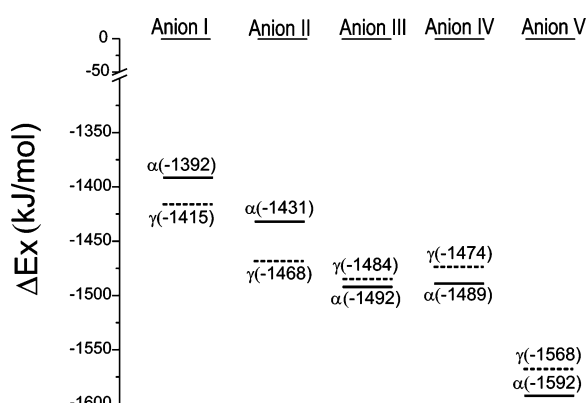
**Table 3.** Reaction Barriers for Four- and Six-Membered Cyclization ( $\Delta E^\ddagger(4)$ ,  $\Delta E^\ddagger(6)$ ,  $\Delta G^\ddagger(4)$ ,  $\Delta G^\ddagger(6)$ ) Expressed in kJ/mol at Various Levels of Theory<sup>a</sup>

level of theory	gas phase results					
	$\Delta E^\ddagger(4)$	$\Delta E^\ddagger(6)$	$\Delta(\Delta E^\ddagger)$	$\Delta G^\ddagger(4)$	$\Delta G^\ddagger(6)$	$\Delta(\Delta G^\ddagger)$
B3LYP/6-311g**//B3LYP/6-311g**	75.72	98.12	22.40	70.28	96.99	26.71
mPW1PW91/6-31+g(d)//B3LYP/6-311g**	91.43	111.69	20.25			
BP86/6-31+g(d)//B3LYP/6-311g**	70.54	86.32	15.78			
B3LYP/6-31+g(d)//B3LYP/6-31+g(d)	81.05	101.83	20.78	75.61	100.70	25.09
B3LYP/6-311+g(d)//B3LYP/6-311+g(d,p)	82.43	103.12	20.69			
mPW1PW91/6-31+g(d)//MPW1PW91/6-311g**	90.78	110.45	19.67	85.34	109.32	23.98

B3LYP/6-31+g(d)//B3LYP/6-31+g(d)	without inclusion of bulk solvent effects			with inclusion of bulk solvent effects		
	$\Delta E^\ddagger(4)$	$\Delta E^\ddagger(6)$	$\Delta(\Delta E^\ddagger)$	$\Delta G^\ddagger(4)$	$\Delta G^\ddagger(6)$	$\Delta(\Delta G^\ddagger)$
transmetalated structures (Na)	157.14	160.54	3.40	95.31	121.45	26.14
transmetalated structures (Li)	167.66	177.65	9.99	102.17	147.31	45.13
transmetalated structures (Na) + 1DME molecule	149.69	140.75	-8.94	88.00	103.31	15.31
transmetalated structures (Na) + 2DME molecule	145.06	140.39	-4.66	58.78	85.62	26.84

<sup>a</sup>  $\Delta(\Delta E^\ddagger)$  is the difference between the reaction barrier for six- and four-membered ring formation, i.e.  $\Delta E^\ddagger(4) - \Delta E^\ddagger(6)$ . In the notation Level1//Level2, Level1 is the electronic level of theory used for the energetics, whereas Level2 is the level of theory used for the geometry optimization.

**Figure 3.** Protonation energies ( $\Delta E_x$ ) for various anions (B3LYP/6-31+g(d) level).

chemically active area of the molecule. The  $C_5-C_1$  and  $C_5-C_3$  distances are not considerably altered. This conclusion also holds for the  $C_2C_1NC_4$  dihedral angle which determines the position of the  $C_5-C_1$  unit to the allylic system. This proves that the counterion exerts limited influence on the structural parameters of the system under consideration.

**Effect of Solvation.** The computations discussed thus far refer to unsolvated compounds. However, THF was used as solvent in our experiments, and solvation may be expected to be important in these ether-like solvents. The solvation originates from two contributions: coordination of ether oxygens to the sodium cation (coordination solvation) and the electrostatic effect of the solvent dielectric medium (dielectric solvation). The latter effect is more easily to deal with from a computational point of view as it is usually approximated by enclosing the molecule in a cavity within a continuous dielectric medium. Recently, an article by Kelly, Cramer, and Truhlar appeared on the accurate determination of solvation free energies, which may be interesting for a more detailed reading on this subject.<sup>50</sup> The dielectric solvation energies (DSE) were obtained using a CPCM (also known as COSMO) option in Gaussian 03 on the unsolvated B3LYP/6-31+g(d) structures.<sup>51</sup> The coordination

solvation energy (CSE) is estimated by coordinating the sodium ion to one or more ether oxygens. Dimethyl ether (DME) was chosen as the coordinating solvent instead of THF. DME has about the same basicity as THF but is significantly smaller for computations. An important question concerns the degree of coordination. For solvent-separated ion pairs, four-coordinated lithium cations have been recognized in NMR studies.<sup>52,53</sup> However, for contact ion pairs as encountered here, the degree of coordination may be dependent on the nature of the counterion, and the coordination may be expected to be smaller due to its electrostatic effect.<sup>54</sup> The degree of coordination for the system under consideration is estimated by coordinating the sodium cation with one, two, three, or four DME molecules and calculating the CSE energies. These values are shown in Figure 1. Coordination of the first two ether molecules is highly exothermic (CSE amounts to  $-53.8$  and  $-88.7$  kJ/mol). As the coordination with the second DME is still highly exothermic, an additional DME molecule was placed close to the ion pair. Coordination of the third DME molecule causes only a slight additional stabilization ( $-98.9$  kJ/mol versus  $-88.7$  kJ/mol) and is located at a large distance of  $4.74$  Å from the sodium ion (compared with Na-O distances of  $2.17$  and  $2.18$  Å for the first two DME molecules). The CSE amounts to  $-102.7$  kJ/mol for four DME molecules, indicating that the coordination effectiveness is largely reduced from the third DME molecule on.

The DSE is obtained as the sum of two terms, an electrostatic term, which has a negative sign and which is derived from the interaction of the solute charges with the solvent, and a nonelectrostatic term, that is generally positive and consisting of the free energy needed for the formation of the cavity in the continuum, a dispersion term and a repulsion term. The value for the DSE on the monomeric ion pair formed by the anion and the sodium ion amounts to  $12.22$  kJ/mol and is non-negligible. These values are in line with the numbers reported by Pratt and Streitwieser.<sup>21</sup> The geometrical parameters with

(50) Kelly, C. P.; Cramer, C. J.; Truhlar, D. G. *J. Chem. Theory Comput.* **2005**, *1*, 1133–1152.

(51) (a) Cossi, M.; Rega, N.; Scalmani, G.; Barone, V. *J. Comput. Chem.* **2003**, *24*, 669–681. (b) Barone, V.; Cossi, M. *J. Phys. Chem. A* **1998**, *102*, 1995–2001.

(52) Reich, H. J.; Green, D. P.; Medina, M. A.; Goldenberg, W. S.; Gudmundsson, B. O.; Dykstra, R. R.; Philips, N. H. *J. Am. Chem. Soc.* **1998**, *120*, 7201–7210.

(53) Carlier, P. R.; Lo, C. W.-S. *J. Am. Chem. Soc.* **2000**, *122*, 12819–12823.

(54) Schade, C.; Schleyer, P. V. R. *Adv. Organomet. Chem.* **1988**, *27*, 169–170.

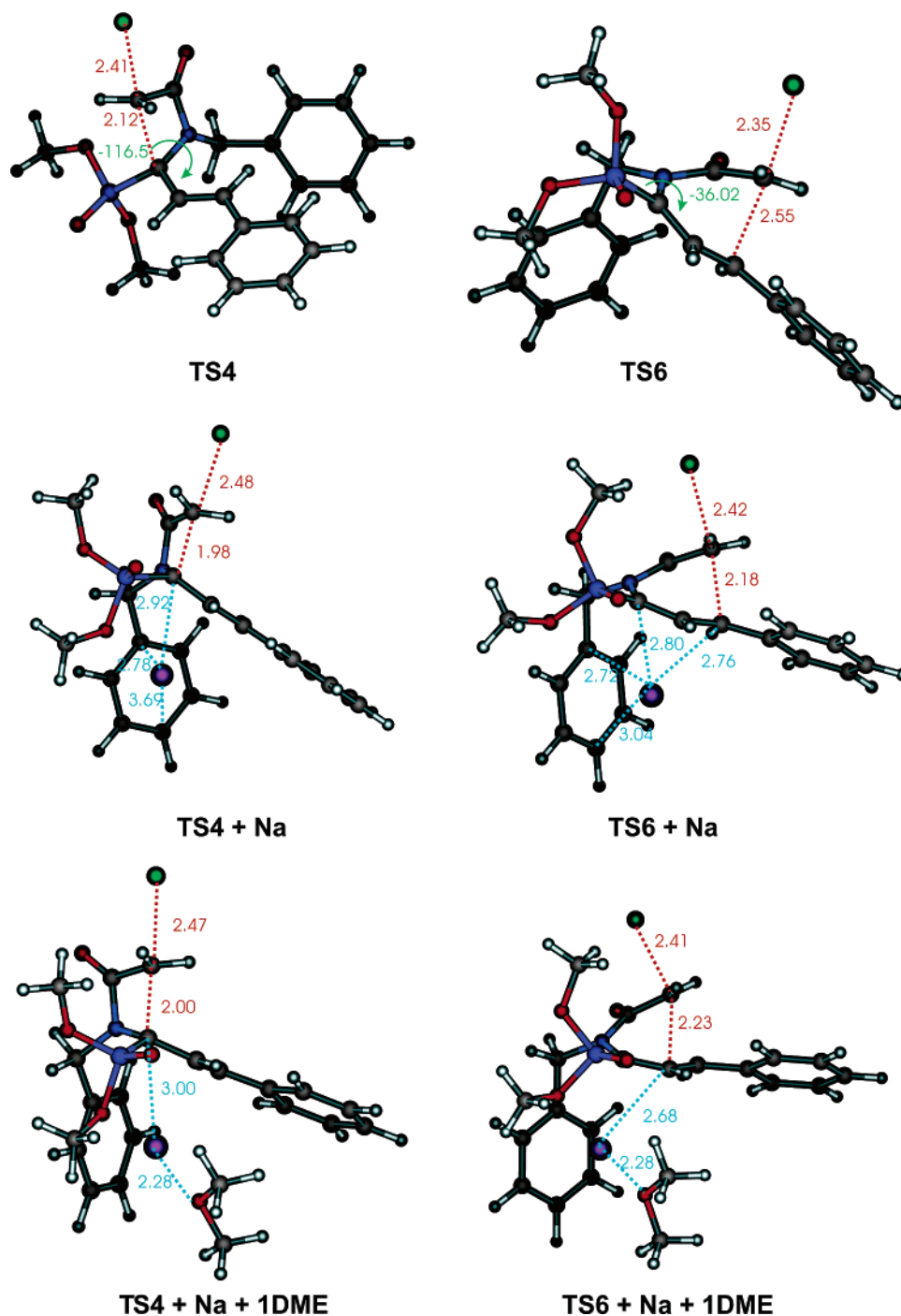


**Figure 4.** Optimized conformers of the transition states in different molecular environments: TS4 and TS6 transition states for four- and six-membered lactam formation in the gas phase; TS4+Na and TS6+Na including one sodium ion; TS4+Na+1DME and TS6+Na+1DME including one sodium ion and one DME molecule. All optimizations are performed at the B3LYP/6-31+g(d) level.

inclusion of solvent molecules, confirm once more that the chemical active area for cyclization remains nearly the same.

**Transition-State Structures.** To unravel the experimentally obtained reaction preference toward four-membered lactams, calculations are performed to determine the reaction barriers. The transition states toward four- and six-membered ring formation in the gas phase are visualized in Figure 4, and some relevant geometrical parameters are given in Table 1.

Both transition states resemble an intramolecular  $S_N2$ -like reaction characterized by an umbrella-like inversion at  $C_5$ . In the reacting anion the  $C_5$  carbon atom is oriented toward the

$\alpha$ -carbon atom, i.e. the reactive center for four-membered ring formation. In the case of six-membered ring formation large distortions are needed from the original geometry of the anion to adapt the  $S_N2$ -like transition structure (cf. Table 1): the dihedral angle  $C_2C_1NC_4$  varies from  $-82.2$  to  $-36.0^\circ$ . To get an idea about energetic variations associated with these distortions, the rotational potential in terms of this geometrical variable was calculated. This was done by a stepwise variation of the  $C_2C_1NC_4$  torsional angle and optimizing all other degrees of freedom. To reduce the computational cost, the B3LYP/3-21+g(d) level of theory was adapted. The results are shown



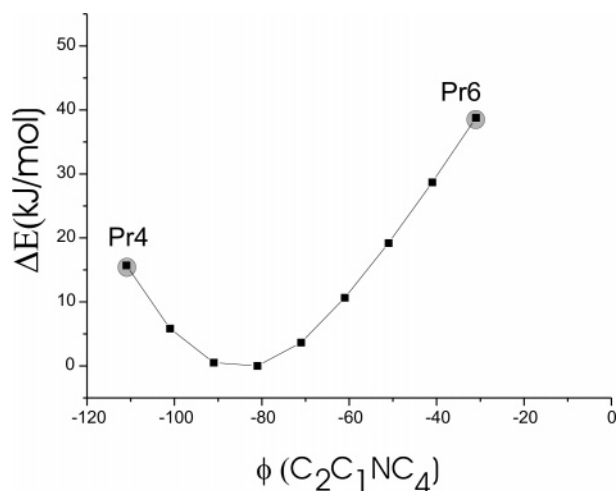


**Figure 5.** Part of the rotational potential in terms of the  $C_2C_1NC_4$  dihedral angle. The precursors for four- and six-membered ring formation (Pr4 and Pr6) are indicated by a gray circle.

in Figure 5 for the appropriate range of the dihedral angle. Starting from the most stable favorable conformation ( $\phi = -82.9^\circ$ ) the torsional angle reaches values of  $-116$  and  $-36^\circ$  in the four- or six-membered transition states, respectively (cf. Table 1). Due to the strongly asymmetric shape of the rotational potential around the minimum, the associated energy to induce such distortions amounts to approximately 15 and 38 kJ/mol. Therefore, a large amount of energy is needed to reach the transition state toward the six-membered lactams. The structures of the transition states with incorporation of the counterions are also visualized in Figure 4. The chemically active part for the ring-closure reaction is not altered substantially; only the phenyl groups slightly relax in the presence of the sodium cation. Furthermore, the distances of the forming C–C bond are shorter ( $\sim 0.15$  Å) at all levels of theory. This is in accordance with the results of Ando.<sup>23</sup>

**Reaction Barriers.** In the further course of the discussion, both the bare reaction barriers  $\Delta E^\ddagger$  (i.e. the electronic energy differences between transition state and corresponding reactant) and the corresponding free energies ( $\Delta G^\ddagger$ ) including zero-point, thermal, and entropic contributions are evaluated. When PCM computations are used, the energies have the status of free energies, since they implicitly take into account the thermal and entropic contributions of the solvent.<sup>55</sup> The values are given in Table 3 at various levels of theory.

First, the influence of the level of theory on the energetic results is discussed. It is generally known that B3LYP geometries are quite accurate<sup>19,42,56</sup> and that variations on the reaction barriers are small by adopting another level for the geometry optimization. This is confirmed by our calculations: mPW1PW91/6-31+g(d)//B3LYP/6-311 g\*\* and mPW1PW91/6-31+g(d)//mPW1PW91/6-31+g(d) predict barriers for four-membered cyclization of 91.43 and 90.78 kJ/mol, respectively. The functional form has a much larger influence on the reaction barriers leading to respective values between 70 to 91 kJ/mol. The selection of the most suitable level of theory is jeopardized by the lack of direct experimental data on the reaction barriers. However, the differences between the reaction barriers for four-

and six-membered ring formation (i.e.  $\Delta(\Delta E^\ddagger) = \Delta E^\ddagger(6) - \Delta E^\ddagger(4)$ , where  $\Delta E^\ddagger(4)$  and  $\Delta E^\ddagger(6)$  are the barriers for four- and six-membered cyclization) show much less variation (16–22 kJ/mol, depending on the electronic level of theory used), predicting a large preference for four-membered ring formation at all levels of theory. The reason for this preference must be traced back to the high amount of energy needed to reach a conformation suitable for six-membered ring formation (cf. Figure 5).

At second instance, the influence of the cation and solvent effects on the reaction barriers is discussed. Inclusion of the sodium cation has a dramatic influence on the reaction barriers. Both barriers increase with approximately 60–80 kJ/mol at all levels of theory. Similar findings were found by Ando.<sup>23</sup> Moreover, there is not a clear preference anymore for four- or six-membered ring formation ( $\Delta(\Delta E^\ddagger) = 3.4$  kJ/mol). However, since the reactions were performed in THF, solvation of the counterion is expected to be important. At first, bulk solvent effects are taken into account using the CPCM model, lowering the reaction barriers to about 95 and 121 kJ/mol (at the B3LYP/6-31+g(d)//B3LYP/6-31+g(d) level) for four- and six-membered ring formation, respectively. Furthermore, the preference for cyclization at the  $\alpha$ -position is correctly predicted by including bulk solvent effects ( $\Delta(\Delta G^\ddagger) = 26.1$  kJ/mol) and thus emphasizing the necessity to treat solvent effects in a proper way.

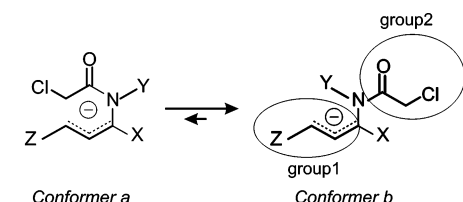
Finally explicit solvent molecules were taken into account as explained previously. The barriers were calculated for one and two DME molecules. Oncemore, inclusion of bulk solvent effects is required to predict the correct reaction preference. The difference between the activation free energy for four- and six-membered ring formation ( $\Delta(\Delta G^\ddagger)$ ) amounts to 15.31 and 26.84 kJ/mol in the case of adding one or two DME molecules, respectively. The value of  $\Delta(\Delta G^\ddagger)$  may be expected to alter only slightly with inclusion of more DME molecules, consistently with the result found for the CSE values. All theoretical calculations are now consistent, explaining the four-membered ring preference. The values of  $\Delta(\Delta G^\ddagger)$  amount to 25.09, 26.14, and 26.84 kJ/mol at the B3LYP/6-31+g(d) level for the gas-phase computations, the calculations with inclusion of the sodium counterion and the inclusion of the sodium and two DME molecules, respectively.

Summarizing, for this particular reaction a correct qualitative picture is predicted using the gas-phase computations. Solvent effects do alter the absolute values of the reaction barriers but do not affect the global  $\alpha/\gamma$  selectivity. This might be anticipated as the geometries of the chemical active part of the system are not significantly altered by inclusion of the molecular environment. However, based on this single application, these conclusions may not be generalized.

**Origin of the Four-Membered Ring Preference.** Finally, suggestions are validated to unravel the true origin of the four-membered ring formation preference. As already pointed out, the rotation about the C–N bond is largely hindered. Moreover the associated potential is asymmetric, i.e. a rotation toward the  $\gamma$ -carbon atom is disfavored (cf. Figure 5). To investigate more in depth these energetically unfavorable effects, the reaction barriers for a number of allyl-stabilized anions differing in the substituents X, Y, and Z attached at various positions of the anion (cf. Figure 6) were calculated.

(55) Tomasi, J.; Persico, M. *Chem. Rev.* **1994**, *94*, 2027–2094.

(56) Gomez-Balderas, R.; Coote, M. L.; Henry, D. J.; Radom, L. *J. Phys. Chem. A* **2004**, *108*, 2874–2883.



	X	Y	Z	$\Delta(\Delta G^\ddagger)$
<b>ANION I</b>	$\text{P}(\text{OMe})_2$	$\text{CH}_2(\text{C}_6\text{H}_5)$	$\text{C}_6\text{H}_5$	26.84
<b>ANION Ia</b>	$\text{P}(\text{OMe})_2$	$\text{CH}_2(\text{C}_6\text{H}_5)$	$\text{CH}_3$	33.97
<b>ANION Ib</b>	$\text{P}(\text{OH})_2$	$\text{CH}_2(\text{C}_6\text{H}_5)$	$\text{C}_6\text{H}_5$	33.21
<b>ANION Ic</b>	$\text{P}(\text{H})_2$	$\text{CH}_2(\text{C}_6\text{H}_5)$	$\text{C}_6\text{H}_5$	20.40
<b>ANION Id</b>	$\text{C}(\text{CH}_3)_2$	$\text{CH}_2(\text{C}_6\text{H}_5)$	$\text{C}_6\text{H}_5$	26.13
<b>ANION Ie</b>	$\text{CH}_3$	$\text{CH}_2(\text{C}_6\text{H}_5)$	$\text{C}_6\text{H}_5$	21.16
<b>ANION If</b>	$\text{CH}_3$	$\text{CH}_3$	$\text{C}_6\text{H}_5$	7.90
<b>ANION Ig</b>	$\text{CH}_3$	$\text{CH}_3$	$\text{CH}_3$	18.81
<b>ANION Ih</b>	$\text{CH}_3$	$\text{CH}_3$	H	26.01

**Figure 6.** Difference between four- and six-membered activation free energies for a variety of allyl stabilized anion. The calculations are performed at the B3LYP/6-31+g(d)/B3LYP/6-31+g(d) level of theory. For Anions I, Ic, Id and Ie also two DME molecules and bulk solvent effects were included.

When substituting the bulky phosphonate group by a tertiary butyl group which is approximately as voluminous, the four-membered ring is still preferred by 26.13 kJ/mol (Anion Id). This indicates that the true nature of the four-membered ring formation preference is not related to the specific properties of the phosphonate group. Nevertheless, the phosphonate group plays a crucial role in the anion stability, allowing selective deprotonation of the substrates. Also Bossio et al. and Marccacini et al. found preference for four-membered ring formation in the case where the anion was stabilized by a carbonyl group.<sup>9,10</sup> Even when substantially reducing the size of the X and Y substituent, four-membered rings are always preferentially formed. This indicates that the size of the X and Y group are not the primary cause for the largely hindered rotation about the C–N bond. The anion can exist in at least two conformers which are schematically shown in Figure 6 and which differ in the relative orientation of the groups 1 and 2 which are attached to the nitrogen–carbon bond. Our calculations point out that Conformer a, which is ready for six-membered ring formation, is highly unstable due to the large amount of energy needed to bring the groups 1 and 2 closer toward each other.

Furthermore, it was investigated whether the site selectivity seen in the reactive anion under study can further be rationalized by inspecting appropriate DFT-based reactivity indicators. Therefore, a variety of global and local indices, such as the global hardness ( $\eta$ ), local softness ( $s(r)$ ), and Fukui function ( $f(r)$ ), were applied to the most stable conformer. For more explanation on their definitions we refer to the textbook of Parr and Yang<sup>39</sup> and a review by Geerlings et al.<sup>57</sup> The reactions studied here concern an ambident nucleophile, where the soft and hard centers are located in the same system. Moreover, the reactions are intramolecular  $\text{S}_{\text{N}}2$  cyclization reactions, and the Fukui function for electrophilic attack ( $\bar{f}(r)$ ) is believed to indicate the most favorable site. The condensed Fukui and

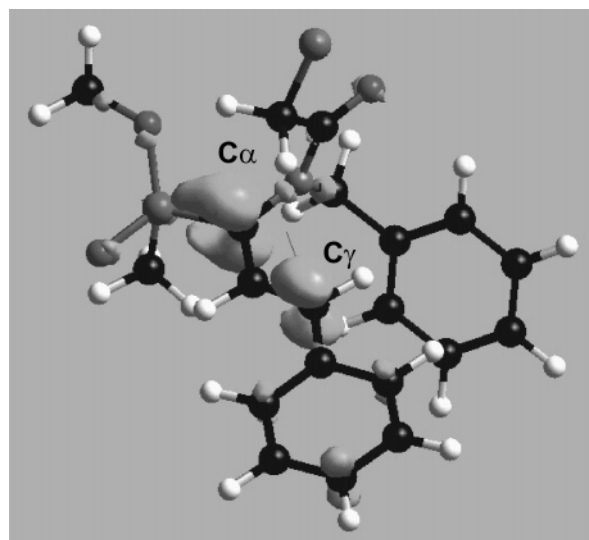


**Figure 7.** Iso-surfaces (value 0.005) of the Fukui function ( $\bar{f}(r)$ ) for electrophilic attack in the most stable conformer of the anion, which is the precursor for four-membered ring formation.

softness values calculated using the natural population analysis (NPA) and CHELPG scheme are given in Table S1 of the Supporting Information. The  $\alpha$ -carbon atom is the softest center, whereas the  $\gamma$ -carbon atom is somewhat harder; thus, the condensed local indices indeed predict that cyclization preferentially occurs at the  $\alpha$ -position. This can further be illustrated by visualizing  $\bar{f}(r)$  of the reactive anion (Figure 7). The largest value for the Fukui function is indeed found at the  $\alpha$ -carbon atom. The specific reaction is an example of a reaction which is frontier-orbital controlled, and the Fukui function is an appropriate indicator to describe the site selectivity.<sup>58,59</sup> The specific selectivity encountered here has been seen in various other systems such as HCHO, NCS, and malonaldehyde anion.<sup>60</sup>

In the anion trapping experiment with a proton, which is known to be very hard, the reaction may be expected to occur preferentially at the hardest center, which is the  $\gamma$ -carbon atom in our case. However, since the alkylation with methyl iodide which is a soft electrophile, also occurs at the  $\gamma$ -position, it can be concluded that the site-selectivity is primarily dictated by geometric constraints, whereas the frontier-orbital interactions are of minor importance.

Summarizing, the four-membered ring preference is due to a largely hindered internal rotation around the C–N bond of the 1-aminoalkenyl-phosphonate, which prevents the anion in reaching the conformer suitable for six-membered ring formation.

## 5. Conclusions

In this study a peculiar ring closure of functionalized aminophosphonates toward four-membered phosphono- $\beta$ -lactams has been unraveled both on experimental and theoretical bases. Starting from an ambident allylic anion, no trace of six-membered lactams was found, and only the highly strained four-membered rings are formed through intramolecular alkylation. Nevertheless, new anion trapping experiments indicate that the

(58) Chattaraj, P. K. *J. Phys. Chem. A* **2001**, *105*, 511–513.

(59) Fukui, F. *Theory of Orientation and Stereoselection*; Springer-Verlag: Berlin, 1973; p 134; *Science* (Washington, D.C.) **1982**, *218*, 747.

(60) Pearson, R. G. *Chemical Hardness: Applications from Molecules to Solids*; Wiley-VCH Verlag GmbH: Weinheim, 1997.

(57) Geerlings, P.; De Proft, F.; Langenaeker, W. *Chem. Rev.* **2003**, *103*, 1793.

$\gamma$ -position is more reactive in intermolecular reactions. This was confirmed by the calculation of theoretical protonation energies, which ascribe the stabilization of this isomer to the presence of the phosphonate- and nitrogen-containing subgroup. However, it was found that the remarkable selectivity is typically associated with intramolecular reactions and was primarily due to a restricted rotation around the C–N bond of the 1-amino-alkenyl-phosphonate studied. Therefore, the transition state for six-membered ring formation is energetically disfavored. The typical  $\text{SN}_2$ -like transition state is geometrically strained for six-membered ring formation and consequently substantially (approximately 25 kJ/mol) more activated. The system of interest is challenging as it contains solvated sodium or lithium ions.

However, the  $\alpha/\gamma$ -selectivity is not notably influenced by accounting for solvent effects.

**Acknowledgment.** This work is supported by the Fund for Scientific Research-Flanders (FWO) and the Research Council of Ghent University.

**Supporting Information Available:** Complete ref 38, reactivity indices for the reactive anion, structural characterization of all compounds, Cartesian coordinates of all optimized reactants, transition structures. This material is available free of charge via the Internet at <http://pubs.acs.org>.

JA0584119